Scott, S. J., Capuzzi, M., Langston, D., Bossanyi, E. A., McCann, G., Weaver, P., & Pirrera, A. (2016). Gust response of aeroelastically tailored wind turbines. Journal of Physics: Conference Series, 753(C), [042006]. DOI: 10.1088/1742-6596/753/4/042006

Gust response of aeroelastically tailored wind turbines

2016 J. Phys.: Conf. Ser. 753 042006

(http://iopscience.iop.org/1742-6596/753/4/042006)

Gust response of aeroelastically tailored wind turbines

S Scott[1], M Capuzzi[1], D Langston[2], E Bossanyi[2], G McCann[2], PM Weaver[1] and A Pirrera[1]

[1] Advanced Composites Centre for Innovation and Science (ACCIS), Department of Aerospace Engineering, University of Bristol, Queen's Building, University Walk, BS8 1TR, UK
[2] DNV GL, One Linear Park, Avon Street, Bristol, BS2 0PS, UK

E-mail: alberto.pirrera@bristol.ac.uk

Abstract. Some interesting challenges arise from the drive to build larger, more durable rotors that produce cheaper energy. The rationale is that, with current wind turbine designs, the power generated is theoretically proportional to the square of blade length. One enabling technology is aeroelastic tailoring that offers enhanced combined energy capture and system durability. The design of two adaptive, aeroelastically tailored blade configurations is considered here. One uses material bend-twist coupling; the other combines both material and geometric coupling. Each structural design meets a predefined coupling distribution, whilst approximately matching the stiffness of an uncoupled baseline blade. A gust analysis shows beneficial flapwise load alleviation for both adaptive blades, with the additional benefits of smoothing variations in electrical power and rotational speed.

1. Background

There is a growing trend in the wind turbine industry towards larger rotors, due to their capacity for greater energy capture. This trend is part of a drive to reduce the overall cost of energy (CoE). However, larger rotors increase aerodynamic and inertial loading which, in turn, places a greater structural demand on blades, drivetrain, tower and foundations. To prevent CoE increases, it is desirable to employ load alleviation strategies, to: (i) extend the lifetime of components, particularly those whose designs are fatigue driven; (ii) reduce the amount of structural material for weight and cost savings; (iii) enable larger rotors for increases in annual energy yield (AEY) for new and retrofitted turbines.

Conventional load management strategy of wind turbines (WTs) employs active pitch control. Alternative ways of achieving load control in a passive manner allow blades to vary their external shape, hence their aerodynamic performance, in response to changing operating conditions. One such way is aeroelastic tailoring that makes use of bend-twist coupling (BTC) to induce twisting of the blade in response to flapwise bending. For example, a gust causes a downwind bending deformation. In a tailored blade, this deformation can induce a nose-down twist such that the blade's angle of attack decreases thus reducing loads. This behaviour gives the blade an inherent load alleviation capability, or passive load control.

Initial studies examined a nose-up twist response for promoting stall, however, such a response is only relevant for stall-regulated turbines and increases fatigue loading [1]. This paper focuses on aeroelastic tailoring that induces a nose-down twist response, as this promotes load alleviation in variable-speed, pitch regulated WTs.

Journal of Physics: Conference Series **753** (2016) 042006 doi:10.1088/1742-6596/753/4/042006

Table 1: DNV GL turbine properties (in-house data).

Rotor orientation/configuration	Upwind, three blades
Control	Variable speed, individual pitch
Rated power (MW)	7
Blade Length (m)	77.7
Cut in, rated, cut out wind speed (ms^{-1})	3, 11, 25
Cut in, rated rotor speed (rpm)	3.98, 10.74

2. Introduction

There are different ways of incorporating BTC into a wind turbine blade that fall into two broad categories: geometric and material coupling [2–8]. Geometric coupling is induced by a curved, or swept, blade planform; material coupling is induced by anisotropic composite materials. Generally, for material coupling, off-axis plies are used to unbalance the composite laminates.

The combination of both material and geometric coupling has been proposed by Capuzzi *et al.* [9–11], where the blade's steady twist deformation at rated is tailored using spatially variable BTC to meet a pre-defined distribution. The prescribed twist distribution is output from an optimisation study, with the objective of maximising energy capture. Specifically, starting from the root, the magnitude of the output nose-down twist angle increases towards the mid-span then decreases towards the tip. This twist curve contrasts with previous work, where only *either* material *or* geometric coupling is used and the magnitude of twist increases monotonically with blade radius. In order to compare the aeroelastic performance of tailored blades featuring monotonic and non-monotonic twist deformations, two design configurations are considered in this work: one with material coupling and one with material *and* geometric coupling. The two adaptive configurations are henceforth referred to as the 'combined-adaptive' (CA) design, due to the use of two couplings, and the 'material-adaptive' (MA) design. Aeroelastically, a design with solely geometric coupling would behave similarly to the MA design. This third case is therefore not taken into consideration. Load alleviation and increases in steady AEY are obtained by Capuzzi *et al.*'s CA design.

This work provides a comparison between the MA and CA blade designs in terms of gust response. A baseline 7 MW WT from DNV GL is used (See table 1), which represents an optimised design, offering a realistic representation of current commercial technology. DNV GL's Bladed is used for the aeroelastic analyses.

3. Twist optimisation study and adaptive blade designs

Similarly to the approach taken by Capuzzi *et al.* [9], the first step in designing the CA blade is a twist optimisation study to maximise blade energy capture through aeroelastic tailoring. In addition, with the introduction of significant elastic twist deflections in the adaptive blades, it can be assumed that using the baseline blade pre-twist distribution is sub-optimal for maximising power production. In [9], Capuzzi *et al.* approach this problem by setting the twist such that

$$\text{pre-twist} = \text{ideal total twist (at rated)} - \text{elastic twist (at rated)},$$

where the ideal total twist is output from the above-mentioned optimisation. This solution offers a 'rated-optimised' design. In this work, however, a single-objective optimisation study is made to find blade twist distributions that maximise AEY.

Structural specifications for the adaptive blades are detailed in section 3.1. Our primary aim is to provide designs that display specific MA or CA twist deflections at rated. Both designs are purposely constrained to maintain stiffness and mass distributions similar to the baseline. This limitation is imposed for comparison purposes, as it ensures limited changes in inertial and

Table 2: Material properties [13].

Material	E-Glass/Epoxy	Foam (F)
E_{11} (GPa)	39.0	0.1
E_{22} (GPa)	8.6	0.1
G_{12} (GPa)	3.8	0.1
ν_{12} (-)	0.28	0.3
ρ (kg m^{-3})	2100.0	100.0

Table 3: Lay-up definitions.

Location	Lay-up
Spar Cap	[θ 45 0 -45 90 90 -45 0 45 θ]
Skin Sandwich	[θ/45/0/-45/90/F/90/-45/0/45/θ]
Shear Web Sandwich	[45/-45/F/-45/45]

elastic properties and, therefore, that operating structural requirements, such as tower clearance, remain satisfied.

To introduce BTC into the MA blade, recommendations from Botasso *et al.* [6] have been followed. As per Capuzzi *et al.* [9–11], for the CA blade, rearward sweep is used to induce a global nose-down coupling, whilst off-axis plies of variable angle are used to vary the amount of coupling. MA solutions are generally associated with small decreases in AEY [6], where the more significant the coupling, the more significant the power loss. In proposing MA and CA designs, this works aims to investigate the relationship between energy capture and load alleviation, and to find out if load alleviation is possible whilst minimising, or even negating, a loss in AEY.

3.1. Structural Design

The structural design process adopted for adaptive blades is now described. Spanwise blade properties are computed using PreComp [12]. The spanwise properties from PreComp are then input into DNV GL's Bladed, and a steady aeroelastic analysis is run to compute the twist deflection at rated wind speed. Bladed models flexible components, including blades, with a modal approach, where the total deformation is a linear combination of mode shapes. Bladed requires a relatively comprehensive WT definition, including all aerodynamic, structural, mechanical and electrical information.

The external geometry of the blade is pre-defined by existing in-house data. For the internal geometry, a conventional configuration is chosen incorporating a single spar box, made up of spar caps and shear webs. Skin sections provide the aerodynamic shape for the leading edge (LE) and trailing edge (TE). The spar caps are made of monolithic composite materials, whilst the shear webs and skins are sandwich panel constructions to avoid buckling. Additionally, the root and tip sections are made entirely of monolithic composite materials. Specifically E-Glass/Epoxy and a medium-density foam are used, with properties shown in table 2. The lay-up definitions for each section are shown in table 3, where θ indicates the off-axis plies and, for the sandwich panels, 'F' indicates the foam core. For simplicity, lay-up definitions and thicknesses are identical between top and bottom spar caps, fore and aft shear webs, and LE and TE sandwich panels. Laminate thicknesses for each design are displayed in figure 1.

To introduce BTC into the MA blade, off-axis plies of constant angle are located in both the spar cap and skins. Similarly to Botasso *et al.* [6], off-axis plies are used only in the outer 70% of the blade span to target maximum aeroelastic benefits while minimising potential weight gain.

Table 4: Total blade mass and percentage differences to the baseline.

	Blade Mass	Difference (%)
B	34725	-
MA	37929	9.23
CA	37282	7.36

Here we use off-axis fibre angles of 9 deg and 7 deg, which were found by trial-and-error to provide useful aeroelastic tailoring benefits, whilst approximately meeting stiffness and distribution of mass of the baseline. For the CA blade, a combination of geometric and material coupling is used, as done by Capuzzi *et al.* [10, 11]. Rearward sweep is used to induce a global nose-down coupling, whilst off-axis plies of variable angle are used to vary the amount of coupling locally. Off-axis plies are placed in both the skin and spar caps, and span the whole length of the blade. These features are displayed in figure 2. Off-axis plies make up between 60-85% of the laminate thicknesses, with generally higher proportions in the spar caps. Small percentages of 90 deg and ± 45 deg fibres are included to account for secondary loading.

In defining the desired CA twist response, a trial-and-error approach is used to find a combination of sweep curvature and fibre angles, with the aim of providing an overall nose-down twist, and maximising the difference between the mid-span and tip twist deflection. The aim for the MA twist deflection is to have a nose-down tip twist of similar magnitude to the mid-span twist of the CA blade. The resulting twist responses, at the WTs' steady-rated wind speeds, are shown in Figure 3. It is noted that specifying the number of blade modes to be used in the aeroelastic calculations is important for capturing accurate torsional dynamics and, in turn, accurate loads and power. Additionally, appropriate blade mesh density is important for correct modal representation. Therefore, 32 stations are used as provided by DNV GL, where mesh convergence has been tested using fatigue loads as the convergence criteria.

Blade masses are displayed in table 4. In this case, there is a mass increase because off-axis plies cause a decrease in global bending stiffness compared to 0 deg fibres. However, it is noted that the proposed designs are not optimal. Weight savings could be made with a refined and/or improved design, potentially including carbon fibre sections in the spar caps. Spar box geometry could also be optimised as described in [14]. However, as this work only aims to provide a top-level structural design, with more emphasis on the results of the gust load studies, blade designs that display the intended coupling behaviour are assumed to be structurally feasible as already shown in [11].

4. Annual Energy Yield

In previous work [9,10], AEY from steady simulations and load alleviation could both be improved for fixed rotor radius, because the baseline employed did not follow the optimal rotor tip-speed ratio. Table 5 shows that, if a WT follows this optimum, aeroelastic tailoring does not offer substantial gains in AEY, at least for fixed rotor radius. Notably, the benefits observed in steady winds are not reflected in results from turbulent simulations, where AEY from 10-min averages is shown to decrease relative to the baseline for the CA blade too. We propose this decrease in AEY is due to the dynamic controller not being re-tuned for the adaptive behaviour (thus lacking the ability to damp higher frequency rotor modes that are excited in the turbulent simulations). This leaves load alleviation as a remaining benefit, which, in turn, could lead to increased AEY by allowing longer blades to be used with little increase in system loads. These considerations suggest that aeroelastic tailoring can be used to reduce CoE by: (a) designing new turbine systems with larger rotors; (b) retrofitting existing turbines with longer blades for a twofold benefit, i.e. reuse of prior tower infrastructure and increased AEY.

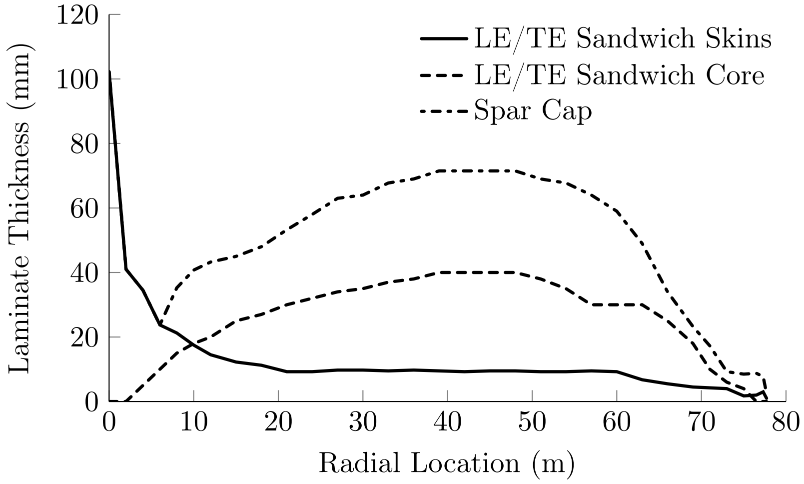

(a) Material-adaptive.

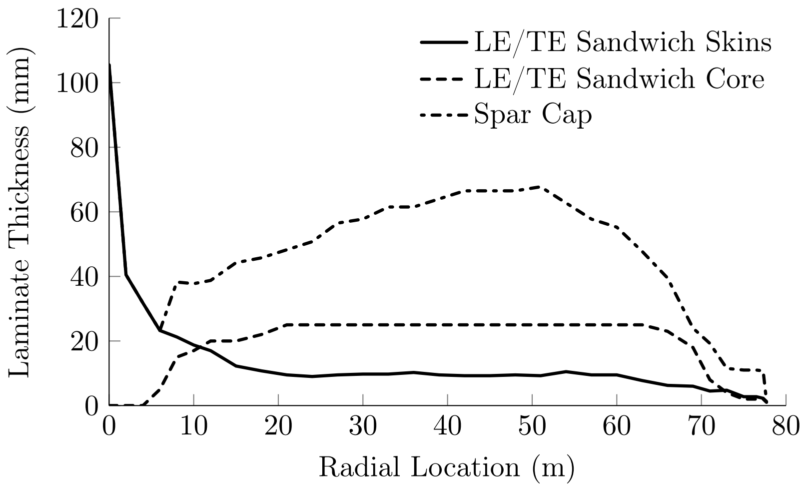

(b) Combined-adaptive.

Figure 1: Laminate thicknesses along the blade length.

Table 5: Steady and turbulent AEY.

	Steady (MWh)	Diff. (%)	Turbulent (MWh)	Diff. (%)
B	25300	-	23524	-
MA	25234	−0.26	23519	−0.02
CA	25394	0.37	23407	−0.49

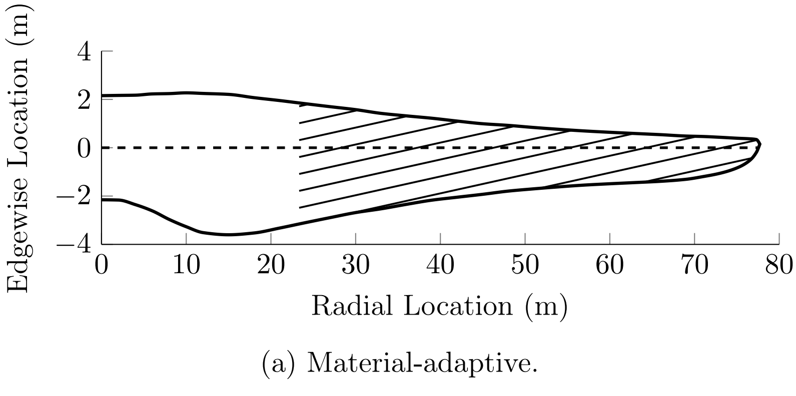

Figure 2: Fibre orientation and sweep curvature.

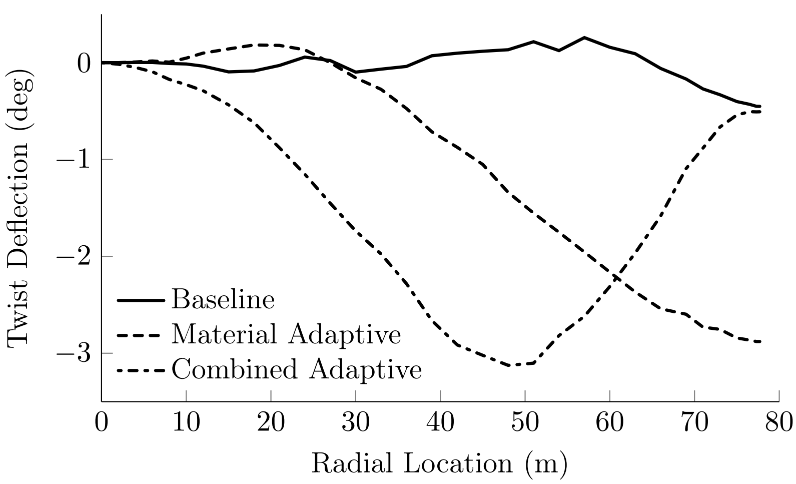

Figure 3: Steady twist deflections at rated wind speed.

Table 6: Gust peak and oscillatory flapwise bending moment and tower root nodding moment.

Load	Location	MA (%)	CA (%)
Peak	Blade Root	−1.95	−4.30
	Tower Root	−2.76	−3.98
Oscillatory (max-min)	Blade Root	−12.03	−15.69
	Tower Root	−9.12	−12.95

5. Gust Analysis

Due to the extreme nature of a gust scenario, the observed response is highly dependant on the blade's adaptive behaviour, which, being elastic in nature, develops almost instantaneously. The dynamic controls are not sufficiently fast to respond to gust and therefore have minimal influence. BTC can be thought of as a kind of inherent material control law that mitigates loads. A gust load solely induces a large coupling response that reacts faster than the pitch system can, thus showing the effectiveness of the adaptive behaviour's potential independently of the controllers.

Dynamic simulations of the WT system are run with an extreme operating gust (EOG) input as specified by the IEC requirements [15]. For a consistent operating regime, the wind speed used is $0.5\,\mathrm{ms}^{-1}$ above rated, guaranteeing the highest loads and the greatest effect from the adaptive behaviour. Both adaptive designs show (see table 6) reductions in peak values and amplitude of oscillation of blade root flapwise bending moment and tower root nodding moment, with the CA performing slightly better. The slightly counter-intuitive result derives from our choice of matching mid-span and tip twist deflections for the MA and CA blades. In fact, it is not possible to generally state that either coupling configuration, material or combined, is more load alleviating than the other; because factors such as the distribution of coupling and the blade's aerodynamic profile influence the location and magnitude of the loads alleviated.

The electrical power signal during the EOG is displayed in figure 4a, where it can be seen that both adaptive designs significantly reduce the power lost in the overshoot, with the CA performing slightly better. Figure 4b displays the variation in rotational speed through the EOG, where peak values and amplitude of oscillation reduce for the adaptive designs. Both results are promising for power output, in terms of power quality to the grid and also reducing the risks of overspeed situations that could result in a shut down. Additionally, the smoothing of rotational speed could reduce the peak stresses in the drivetrain and generator.

6. Conclusions

A comparison of aeroelastically tailored blades is presented, with a focus on gust response. Two adaptive blades are considered, one with material coupling and the other with combined material and geometric coupling. The tailoring capabilities are restricted to negligibly impact the global stiffness and dynamic characteristics of the baseline, so as to provide an appropriate comparison. This restriction causes increases in blade mass. However, adaptive designs generally offer potential for lightweighting due to decreases in loads and thus required stiffness. In addition to load alleviation, gust analyses show smoothing of electrical power and rotational speed, with the CA performing marginally better than the MA. Future work will focus on the effects of aeroelastic tailoring on the pitch and control systems. Preliminary analyses show promising reductions in actuator duty cycle.

Acknowledgments

The authors would like to acknowledge the support of the EPSRC under its SUPERGEN Wind Challenge 2015 Grant, EP/N006127/1.

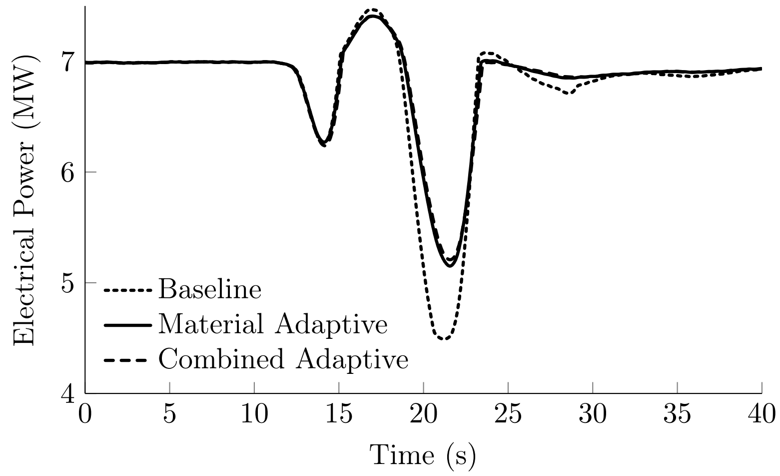

(a) Electrical Power.

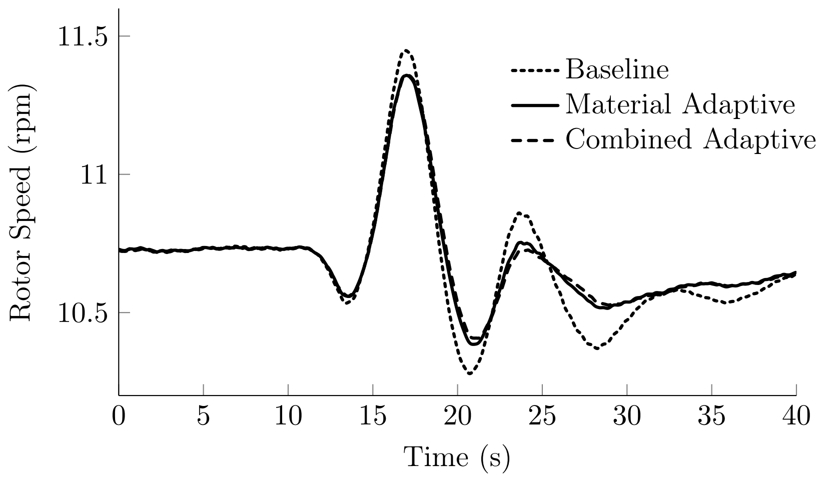

(b) Rotational Speed.

Figure 4: Output results from EOG simulation.

References

[1] Lobitz D W, Veers P S and Migliore P G 1996 *Proc. 1996 ASME Wind Energy Symp. Houston, TX*
[2] Knight & Carver Wind Group 2010 Sweep-Twist Adaptive Rotor Blade. Tech. rep. Sandia Labs
[3] Findlay C July 2013 *Living Energy* 8 (Siemens)
[4] Larwood S, van Dam C P and Schow D 2014 *Renew. Energ.* **71** 563–571
[5] Lobitz D W 2004 *Wind Energy* **7** 211–224
[6] Bottasso C L, Campagnolo F, Croce A and Tibaldi C 2013 *Wind Energy* **16** 1149–1166
[7] Gözcü M O, Olgun M N and Kayran A 2014 *J. Phys.: Conf. Series* **524**
[8] Jonkman J, Butterfield S, Musial W and Scott G 2009 Definition of a 5-MW Reference Wind Turbine for Offshore System Development. Tech. rep. NREL
[9] Capuzzi M, Pirrera A and Weaver P M 2014 *Energy* **73** 15–24
[10] Capuzzi M, Pirrera A and Weaver P M 2014 *Energy* **73** 25–32
[11] Capuzzi M, Pirrera A and Weaver P M 2015 *Thin-Wall. Struct.* **95** 7–15
[12] Bir G S 2005 *User's Guide to PreComp – Pre-Processor for Computing Composite Blade Properties*
[13] Daniel I M and Ishai O 2006 *Engineering Mechanics of Composite Materials* (Oxford University Press)
[14] Pirrera A, Capuzzi M, Buckney N and Weaver P M 2012 *53rd AIAA/ASME/ASCE/AHS/ASC Structures, Structural Dynamics and Materials Conference* (Honolulu, HI) AIAA 2012-1500
[15] 2005 *IEC 61400-1: Wind turbines - Part 1: Design requirements* (IEC)